

Structure-Based Redesign of Cofactor Binding in Putrescine Oxidase

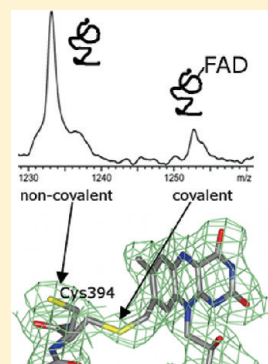
Malgorzata M. Kopacz,[†] Stefano Rovida,[‡] Esther van Duijn,[§] Marco W. Fraaije,^{*,†} and Andrea Mattevi[‡]

[†]Laboratory of Biochemistry, Groningen Biomolecular Sciences and Biotechnology Institute, University of Groningen, Nijenborgh 4, 9747 AG Groningen, The Netherlands

[‡]Department of Genetics and Microbiology, University of Pavia, Via Ferrata 1, 27100 Pavia, Italy

[§]Biomolecular and Mass Spectrometry and Proteomics Group, Utrecht University, Padualaan 8, 3584 CH Utrecht, The Netherlands

ABSTRACT: Putrescine oxidase (PuO) from *Rhodococcus erythropolis* is a soluble homodimeric flavoprotein, which oxidizes small aliphatic diamines. In this study, we report the crystal structures and cofactor binding properties of wild-type and mutant enzymes. From a structural viewpoint, PuO closely resembles the sequence-related human monoamine oxidases A and B. This similarity is striking in the flavin-binding site even if PuO does not covalently bind the cofactor as do the monoamine oxidases. A remarkable conserved feature is the *cis* peptide conformation of the Tyr residue whose conformation is important for substrate recognition in the active site cavity. The structure of PuO in complex with the reaction product reveals that Glu324 is crucial in recognizing the terminal amino group of the diamine substrate and explains the narrow substrate specificity of the enzyme. The structural analysis also provides clues for identification of residues that are responsible for the competitive binding of ADP versus FAD (~50% of wild-type PuO monomers isolated are occupied by ADP instead of FAD). By replacing Pro15, which is part of the dinucleotide-binding domain, enzyme preparations were obtained that are almost 100% in the FAD-bound form. Furthermore, mutants have been designed and prepared that form a covalent 8 α -S-cysteinyl-FAD linkage. These data provide new insights into the molecular basis for substrate recognition in amine oxidases and demonstrate that engineering of flavoenzymes to introduce covalent linkage with the cofactor is a possible route to develop more stable protein molecules, better suited for biocatalytic purposes.



Flavin cofactors FMN and FAD are essential for the catalytic function of a wide range of proteins. In most cases, they are tightly bound to proteins as prosthetic groups by dedicated cofactor-binding domains. Analysis of the available crystal structures of FAD-containing proteins reveals several structural classes.¹ The majority of these FAD-containing proteins contain a distinct domain that binds tightly but in a noncovalent manner the ADP moiety of the FAD molecule. In many cases this is a Rossmann fold dinucleotide-binding domain, which can be easily recognized at sequence level by the canonical GxGxxG sequence motif. Another layer of complexity concerning flavin cofactor binding is added by the observation that some flavoproteins contain a covalently bound flavin cofactor. Several types of covalent protein–FAD linkages have been found.² The most common covalent bond involves the C8 α -methyl moiety of the flavin cofactor and a histidine or cysteine residue. The role of the covalent flavin–protein bond appears to vary from protein to protein. In some flavoproteins the covalent linkage is required in order to tune the redox properties of the flavin or to increase protein stability. Flavin incorporation has been shown to be an autocatalytic process which is in contrast to other covalently bound cofactors, e.g., heme in cytochrome *c*, that depend on dedicated enzymes that catalyze covalent cofactor incorporation.^{3–7}

Putrescine oxidase from *Rhodococcus erythropolis* (PuO) is a recently discovered amine oxidase which contains a noncovalently bound FAD molecule.⁸ It shows a high degree of sequence homology with human and fungal monoamine oxidases (MAOs),

which are all active on a broad range of aromatic compounds.^{9,10} Nevertheless, PuO only accepts a few small aliphatic diamines as substrates, such as putrescine and cadaverine. Protomers of this enzyme are predicted to bind one FAD because of the presence of the typical dinucleotide-binding motif. However, PuO has been found to contain one FAD molecule per protein dimer.^{11,12} Mass spectrometry (MS) analysis has recently revealed that this relatively low FAD content is the result of competitive non-covalent binding of ADP into the FAD binding site. The sequence-related human MAO A and B bind one covalently linked FAD molecule per protomer.¹³ This suggests that in some proteins covalent flavinylation may have evolved to outcompete ADP binding.

In this study, our goal is to identify the residues that tune the cofactor binding properties of PuO. For this, the crystal structures of wild-type PuO and several mutants have been elucidated. Furthermore, electrospray ionization mass spectroscopy (ESI-MS) has been used to determine the FAD and ADP contents and their distribution in the dimeric protein. The structural analysis, together with enzyme kinetic data, reveals that subtle changes in the FAD binding pocket can significantly (1) increase binding of FAD over ADP and (2) lead to efficient covalent incorporation of the FAD cofactor.

Received: March 13, 2011

Revised: April 12, 2011

Published: April 12, 2011

Table 1. Crystallographic Statistics

| | wild-type | product-bound | A394C | P15I/A394C | A394C/A396T/Q431G |
|-------------------------------------|-------------------|-------------------|---------------------|-------------------|---------------------|
| PDB entry | 2yg3 | 2yg4 | 2yg5 | 2yg6 | 2yg7 |
| space group | $P2_12_12$ | $P2_12_12$ | $P4_122$ | $P2_12_12$ | $I2_12_12$ |
| unit cell axes (Å) | 197.6, 79.8, 91.7 | 198.6, 80.6, 92.1 | 102.0, 102.0, 130.4 | 198.4, 80.3, 91.4 | 114.0, 120.4, 171.4 |
| resolution (Å) | 2.0 | 2.3 | 1.9 | 2.5 | 2.7 |
| R_{merge} (%) ^a | 9.5 (31.2) | 12.8 (39.4) | 12.4 (51.2) | 9.7 (24.0) | 14.6 (59.8) |
| completeness (%) ^a | 99.8 (96.2) | 99.8 (99.4) | 99.8 (99.4) | 99.5 (100.0) | 99.8 (99.4) |
| unique reflections | 96 941 | 66 382 | 54 711 | 51 121 | 31 023 |
| multiplicity | 3.7 | 3.8 | 14.5 | 5.0 | 4.1 |
| R_{cryst} (%) | 17.5 | 15.7 | 19.8 | 18.4 | 23.0 |
| R_{free} (%) | 20.1 | 19.9 | 24.2 | 23.1 | 27.6 |
| rmsd bond length (Å) | 0.014 | 0.023 | 0.030 | 0.022 | 0.015 |
| rmsd bond angles (deg) | 1.4 | 2.0 | 2.1 | 1.9 | 1.6 |

^aData for the highest resolution shell are in parentheses.

EXPERIMENTAL PROCEDURES

Chemicals. Oligonucleotides and horseradish peroxidase were from Sigma-Aldrich. *PfuTurbo* DNA polymerase was from Stratagene. *Escherichia coli* TOP10 from Invitrogen was used as a host for DNA manipulations and protein expression. All other chemicals were of analytical grade. Constructs were sequenced at GATC Biotech (Konstanz, Germany).

Construction of PuO P15I/A394C, PuO A394C/V433M, and PuO A394C/A396T/Q431G. The mutants were prepared using the QuikChange site-directed mutagenesis kit from Stratagene. pBAD-PuO_{Rh}A394C¹¹ was the template. The primers used for this are the following:

P15I_{frw}, 5'-GTCGGCGCCGCGCATCTCTGGCCTGG-3';
P15I_{rv}, 5'-CCAGGCCAGAGATGCCGGCGCCGAC-3';
V433M_{frw}, 5'-GAGGGGTACCAGCACATGGACGGTG
CCGTTC-3';
V433M_{rv}, 5'-GAACGGCACCGTCCATGTGCTGGTACC-
CCTC-3';
A396T_{frw}, 5'-CGCGGTTGTTACACGGCGAGCTTCGA
TC-3';
A396T_{rv}, 5'-GATCGAAGCTCGCCGTGTAACAACCGCG-
3';
Q431G_{frw}, 5'-GCCGAGGGGTACGGGCACGTCGACGG-
3';
Q431G_{rv}, 5'-CCGTCGACGTGCCCGTACCCCTCGGC.

The sites of mutation are underlined.

Expression and Purification. Expression and purification of wild-type PuO and its mutants was performed as described before.⁸

FAD Covalent Incorporation Reaction. To monitor FAD—protein covalent bond formation in PuO, enzyme (50 mM Tris-HCl, pH 7.5) was diluted in 50 mM sodium carbonate, pH 10.0 (final pH 8.3), and incubated at 17 °C. No exogenous FAD was added. Samples were taken in time and analyzed for activity and amount for covalent FAD.

ESI-MS Experiments. For nanoflow ESI-MS analysis under native conditions, enzyme samples were prepared in 50 mM ammonium acetate, pH 6.8. For analysis under denaturing conditions, enzyme samples were diluted either in 50% acetonitrile with 0.2% formic acid or in 5% formic acid. Analysis was performed on a LC-T nanoflow ESI orthogonal TOF mass spectrometer (Micromass, Manchester, UK). All measurements were performed by operating in the positive ion mode and by using gold-coated needles, made from borosilicate glass capillaries

(Kwik-Fil; World Precision Instruments, Sarasota) on a P-97 puller (from Sutter Instruments, Novato). The needles were coated with a gold layer, which was performed by an Edwards Scancoat six Pirani 501 sputter coater (Edwards Laboratories, Milpitas). Mass spectra were calibrated using cesium iodide in water (25 mg/mL).

Analytical Methods. Absorbance spectra were recorded in 50 mM Tris-HCl, pH 7.5, or Tris-carbonate, pH 8.3, at 25 °C on a PerkinElmer Lambda Bio40 spectrophotometer. Enzyme concentrations were determined by measurement of absorbance at 280 nm using $\epsilon_{280} = 63\,370\text{ M}^{-1}\text{ cm}^{-1}$ (<http://www.expasy.ch/sprot/>) and recalculated for monomers containing FAD. Oxidase activity was measured by using a coupled horseradish peroxidase assay as described before at pH 8.0.⁸ To measure the noncovalent FAD concentration ($\epsilon_{450} = 11.3\text{ mM}^{-1}\text{ cm}^{-1}$), 5% trichloroacetic acid (TCA) was used to precipitate the protein, and the absorbance spectrum of the supernatant was recorded after centrifugation.

Crystallization and Structure Determination. Crystallization conditions were initially screened using an Oryx8 robot (Douglas Instruments) with 96-well plates. Positive results were obtained in vapor microbatch under a mixture of 70% paraffin—30% silicon oils with ammonium sulfate and PEG400 precipitants. Conditions were further optimized, and crystals of wild-type and mutant enzymes used for structure determination were obtained by the sitting-drop vapor-diffusion method at 4 °C by mixing equal volumes (2–4 μL) of protein and reservoir solutions. Protein solutions consisted of 8–10 mg enzyme/mL in phosphate buffer, pH 7.2, whereas precipitant solutions consisted of 2.0–2.4 M ammonium sulfate, 0.1 M sodium citrate, and 0.1 M Mes-HCl pH 6.4. Structure of the wild-type protein in complex with the reaction product was obtained by soaking a crystal at 20 °C for 1 h in a solution containing 10 mM 1,4-diaminobutane, 2.5 M ammonium sulfate, 0.1 M sodium citrate, and 0.1 M Mes-HCl, pH 6.4.

For data collection, crystals were briefly soaked in a cryoprotectant solution consisting of 20% (v/v) glycerol, 2.5 M ammonium sulfate, 0.1 M sodium citrate, and 0.1 M Mes-HCl pH 6.4. X-ray diffraction data were collected at 100 K at the European Synchrotron Radiation Facility in Grenoble (France) and Swiss Light Source in Villigen (Switzerland). Images were processed using the CCP4 suite programs.¹⁴ The structure of the wild-type enzyme was solved by molecular replacement using the structure of a monomer of MAO B as search model (Protein Data Bank entry 2VSZ).

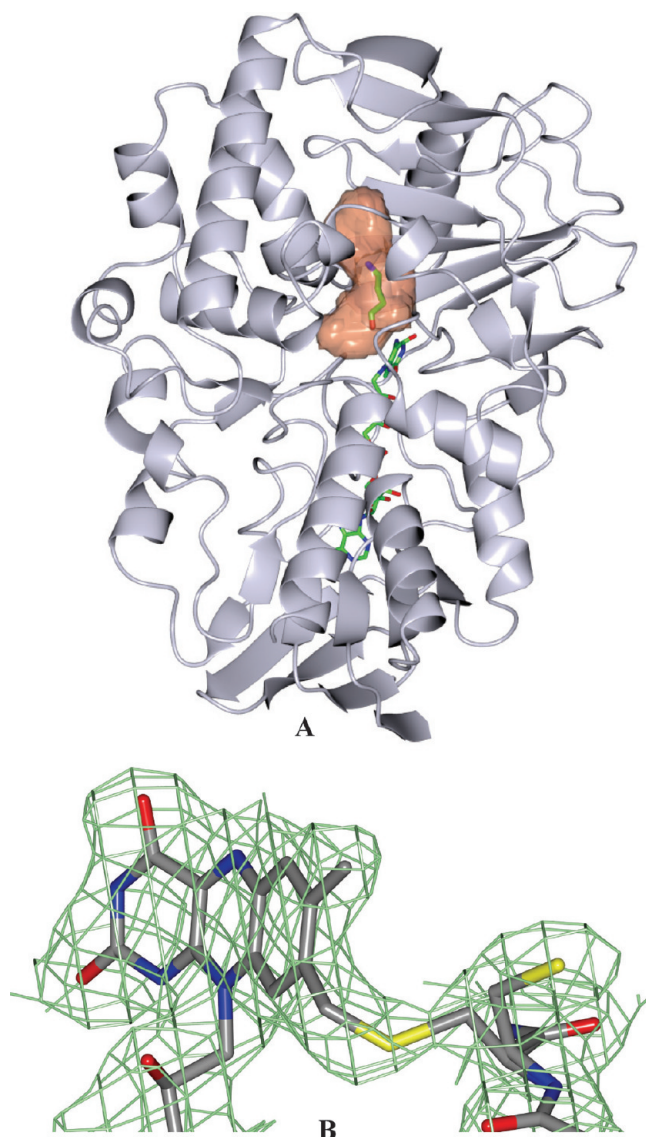


Figure 1. Overall structure of PuO and quality of the crystallographic data. (A) The protein exhibits the same folding topology as MAOs. FAD and bound 4-aminobutanal are shown as ball-and-sticks with carbons in green, oxygens in red, nitrogens in blue, and phosphorus atoms in magenta. The active site cavity is outlined as a semitransparent red surface. (B) Crystallographic data for the P151/A394C PuO mutant structure (subunit B). The picture shows the final weighted $2F_o - F_c$ electron density map for the flavin ring and the double conformation of Cys394. The contour level is 1σ . Oxygens are in red, nitrogens in blue, phosphorus atoms in magenta, carbons in gray, and sulfurs in yellow.

All other PuO structures were solved by molecular replacement employing the wild-type structure as search model. Crystallographic computing and model analysis were performed with COOT¹⁵ and programs of the CCP4 package.¹⁴ Pictures were generated with the program CCP4mg.¹⁶ Cavity calculations were performed with the program VOIDOO.¹⁷ Data collection parameters and final refinement statistics are listed in Table 1.

RESULTS

Structural Properties of Wild-Type PuO. PuO is a stable protein which crystallizes quite readily, yielding different crystal

forms (Table 1). Structure determinations and refinements were done following standard crystallographic protocols, taking advantage of the good quality of the diffraction data which produced excellent electron density maps. All protein residues (except the N-terminal first amino acid and the C-terminal 3–4 residues) have well-defined ordered conformations. Atomic superpositions indicate that the conformations of the crystallographically independent protein subunits are highly conserved across different crystal forms as shown by root-mean-square deviations in the range of 0.1–0.3 Å (using C α atoms). This observation implies that both ligand binding and side-chain mutations cause minimal or no conformational changes with respect to the native wild-type enzyme. On this basis, unless otherwise stated, model analysis was carried out with reference to the A subunit of the ligand-bound structure obtained by soaking the crystals in a putrescine-containing solution (Figure 1A). With the exception of the A394C/A396T/Q431G triple mutant (see below), the flavin ring of FAD exhibits well-defined electron densities and was refined with full occupancy (Figure 1B). This indicates that the FAD-bound (rather than ADP-bound) enzyme molecules are preferentially incorporated into the crystals because of more ordered and/or rigid conformations.

The overall structure of PuO is similar to those of human MAO A and MAO B, which represent the closest structural homologues present in the Protein Data Bank^{9,18,19} (Figure 1A). Atomic superpositions yield root-mean-square deviations of 1.7 and 1.6 Å for 439 and 445 C α atoms with 30% and 33% sequence identities, respectively. The comparative analysis indicates that PuO and MAOs share a generally similar backbone conformation with local conformational variations but no large alterations due to insertions/deletions or large shifts of secondary structures. Furthermore, PuO forms the same dimeric structure as found in human MAO B consistent with its elution profile on size-exclusion chromatography and MS data.¹¹

Despite such a clear relation with human MAOs, analysis of the PuO structure highlights several interesting features, which deserve a closer description. A first intriguing point is the remarkable similarity between the FAD-binding sites of PuO and human MAOs A and B. The conformations of the MAO residues involved in the covalent bond with the flavin are very similar to those of the corresponding region of PuO in which Ala394 replaces the flavinylated Cys of MAOs (Figure 2A). This feature is particularly noticeable, because the flavinylated Cys of MAOs is connected to a Tyr residue through a conformationally unfavorable *cis* peptide bond. Such a Cys–Tyr motif of MAOs is replaced by Ala394–Tyr395 in PuO, which, strikingly, exhibits the same *cis* peptide bond. As a result, Ala394 is positioned close to the C8 α -methyl group of the flavin, which has important implications for generating a site for covalent flavinylation in PuO, as described below (Figure 2).

Another interesting feature concerns the active site. Soaking the crystals in a putrescine-containing solution led to a well-defined electron density peak, which can be perfectly fitted by a linear six-atom ligand. We modeled this compound as 4-aminobutanal, assuming that the complex corresponds to the product-bound enzyme (Figure 3). However, we cannot rule out that the crystals contain bound putrescine or a mixture of substrate and product. PuO exhibits a cavity in front of the flavin cofactor with a volume of 300 Å³ (Figure 1A). This cavity has a bipartite shape with approximately equal inner and outer chambers. The inner space is occupied by the 4-aminobutanal, which extends across the cavity along a direction orthogonal to the *re*-face of the flavin

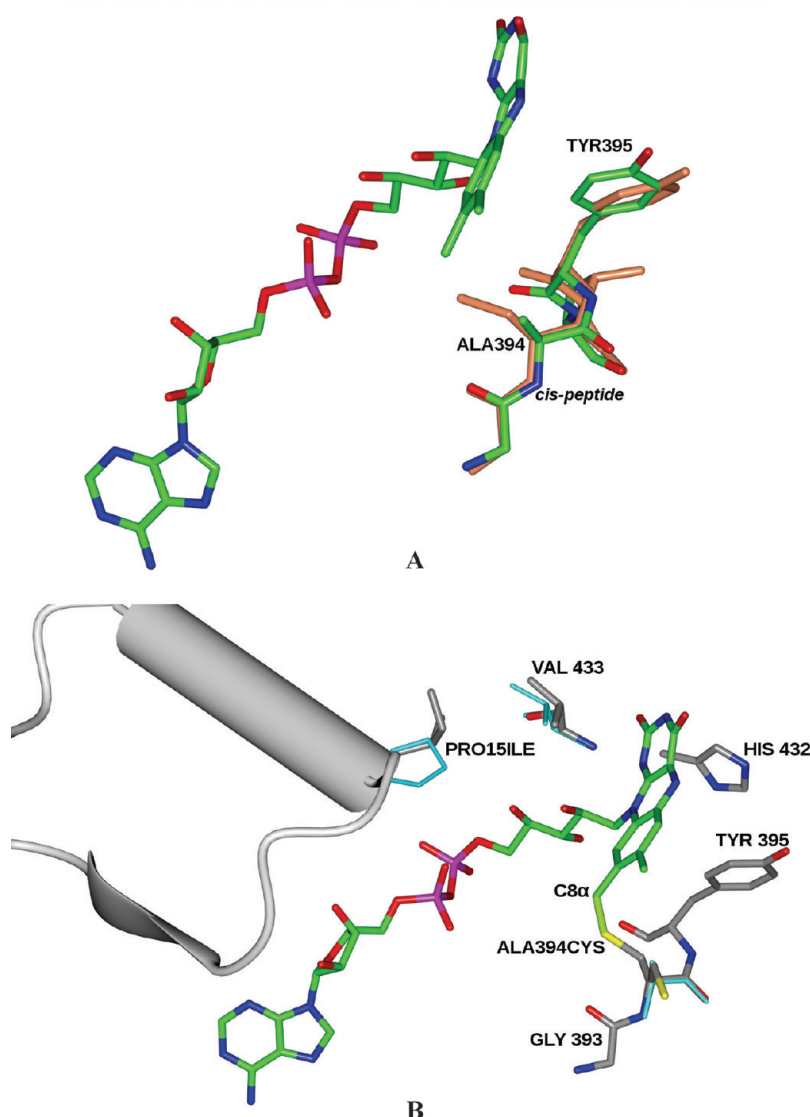


Figure 2. Close-up view of the flavin-binding site of PuO in the same orientation as in Figure 1. (A) Comparison of the structure of wild-type PuO with that of human MAO B. PuO oxygens are in red, nitrogens in blue, phosphorus atoms in magenta, and carbons in green. Gly396, Cys397, Tyr398, and Thr399 of human MAO B are superimposed and show in light brown. (B) Structure of the P15I/A394C PuO mutant (subunit B). Oxygens are in red, nitrogens in blue, phosphorus atoms in magenta, protein carbons in gray, sulfurs in yellow, and FAD carbons in green. Wild-type Pro15, Ala394, and Val433 are superimposed and shown in cyan. Pro15 is located at the N-terminus of the α -helix (shown as cylinder) of the $\beta\alpha\beta$ unit which forms the binding site for the pyrophosphate group of FAD. Ala394 is in contact with the cofactor C8 α -methyl group and is engaged in a *cis* peptide link with Tyr395. The Cys in P15I/A394C mutant has a double conformation, one of them (50% occupancy) forming a covalent bond with the flavin.

ring. As often observed in flavin amine oxidases, the isoalloxazine ring adopts a nonplanar distorted conformation.²⁰ Also Lys296, H-bonded through a water molecule to the N(5) of the FAD (Figure 3), is reminiscent of other flavoprotein oxidase structures. The ligand aldehyde group is in contact with the flavin and is located between the aromatic rings of Tyr395 and His432. These two side chains form an “aromatic sandwich” similar to that of other amine oxidases²⁰ (Figure 3). The only difference is that PuO has a His/Tyr pair rather than the Phe/Tyr or Tyr/Tyr combination found in polyamine oxidase and in MAOs,^{9,10,21} although mutagenesis data has shown that human MAO B retains activity even with a His/Tyr pair as found in PuO.²² The ligand amino group is engaged in H-bonds with the side chain of Glu324 and the carbonyl oxygen of Gly172. These two residues

together with Met173 generate the constriction that separates the two chambers of the active site cavity (Figures 1A and 3). Of particular relevance is the role of Glu324, which functions as a sort of active site ruler that determines the distance between the flavin and the binding site for the positively charged amino group of the substrate. This feature is a key element to explain PuO’s preference for diamino substrates such as putrescine and cadaverine, in which the two amino groups are separated by four and five carbon atoms, respectively. The shape and size of the outer chamber of the cavity extending beyond Glu324 provides additional space for binding an aliphatic substituent on the distal amino group, which is consistent with the ability of PuO to oxidize spermidine (although less efficiently than putrescine; Figure 1A). In summary, PuO is a typical amine oxidase in which

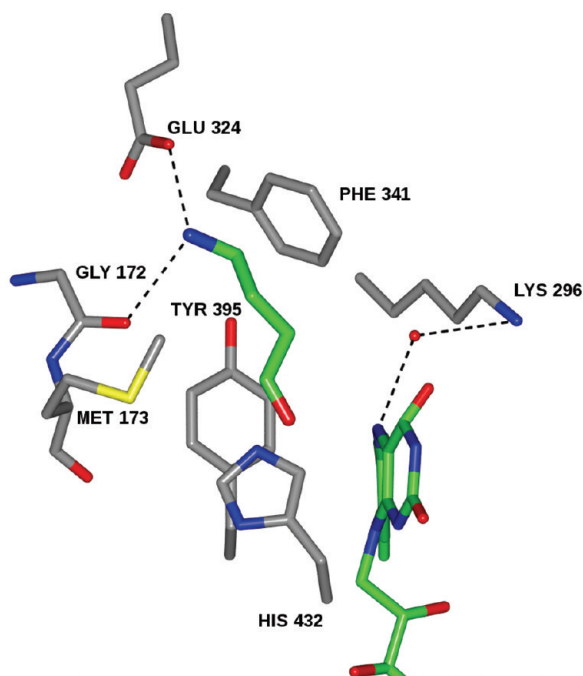


Figure 3. Binding of the active-site ligand present in the structure obtained by crystal soaking in a putrescine-containing solution. The ligand has been tentatively modeled as 4-aminobutanal. Oxygens are in red, nitrogens in blue, protein carbons in gray, FAD and 4-aminobutanal carbons in green. H-bonds are shown as dashed lines.

the local conformation and the nature of the residues surrounding the active-site cavity dictate the enzyme preferences for small aliphatic diamines.

Improving the Affinity toward FAD: P15I/A394C and A394C/V433M. In a previous study, the A394C PuO mutant was constructed, purified, and characterized.¹¹ The introduced cysteine is structurally analogous to the Cys that forms a covalent cysteinyl–FAD linkage in MAO (Figure 2A). The mutant was found to retain activity, but only a marginal fraction (15%) of the mutant protein contained covalently bound FAD, whereas remaining FAD was still dissociable (Tables 2 and 3). In the framework of the present study, we have solved the A394C crystal structure, which turned out to be virtually indistinguishable from that of the wild-type enzyme (Table 1). Cys394 is partly disordered and was modeled in two alternative conformations, with neither of them forming a covalent bond with the flavin. Thus, the crystalline mutant A394C enzyme does not contain covalently bound flavin, at least at a detectable level, which is consistent with the low degree of covalent flavinylation exhibited by the mutant protein (Table 2). On the other hand, the A394C structure clearly indicated that a Cys side chain can be introduced at position 394 without any large structural perturbation, supporting the idea that further amino acid substitutions might render PuO fully capable of efficiently binding FAD in covalent manner.

Therefore, we generated other mutants to enhance flavin binding and efficiency of covalent linkage formation. We compared the PuO structure with those of other dinucleotide-binding domains available through the Protein Data Bank. Generally, these proteins bear low sequence homologies, but all share a GXGXXG phosphate-binding loop which connects the β -strand to the α -helix of the characteristic $\beta\alpha\beta$ unit²³ (Figure 2B). This

dinucleotide-binding motif is not only found in FAD-binding proteins but is also present in ADP-, ATP-, and NAD(P)-binding proteins.²⁴ Inspection of the residues encompassing the dinucleotide-binding motif in PuO reveals an atypical residue, Pro15, next to the second conserved Gly. Sequence comparisons with structurally related FAD-containing amine oxidases reveal that, in most cases, a bulky hydrophobic residue (Phe, Leu, or Ile) is found at this position.²⁵ These observations prompted us to determine whether this residue may play a role in the unique cofactor binding behavior of PuO, which binds FAD and ADP in a 1:1 ratio (Table 2). Thus, P15I/A394C PuO double mutant was produced and its cofactor binding characteristics were analyzed by native ESI-MS.²⁶ Interestingly, the resulting spectrum reveals only two major dimeric species of 99 801 and 100 158 Da (Figure 4). Minor amounts of some other PuO species (3 kDa larger) are likely to be a result of translation by *E. coli* using an alternative stop codon, as observed for wild-type PuO.^{8,11} Analysis of the data showed that the majority of the protein (86%, theoretical mass of 100 152 Da) is present as a dimer containing two FAD molecules (Table 2). The other dominant species (14%, 99 801 Da) corresponds to dimeric PuO containing one FAD and one ADP (theoretical mass of 99 794 Da). No peaks corresponding to apo dimers or dimers with two ADP molecules bound were found. The calculated FAD to ADP ratio in the P15I/A394C mutant is 9–10 times higher than in WT PuO, confirming that the N-terminal Rossmann-fold domain plays a crucial role in facilitating effective FAD binding (Table 2). On the other hand, the P15I/A394C protein did not exhibit any improvement in covalent incorporation of the cofactor since only 16% of the incorporated FAD molecules are covalently bound to the protein (although this value increases to 35% upon prolonged incubation of the protein for 2 days; see below and Table 2 for details).

In order to evaluate the conformational effects of the P15I mutation, the crystal structure of P15I/A394C PuO was determined (Figure 2B). The mutant is virtually identical to the wild-type enzyme with Ile15 overlapping the position of Pro15. The electron density of subunit B (the crystals contain two subunits in the asymmetric unit) indicates that a significant fraction of the protein molecules contain Cys394 covalently bound to the flavin C8 α atom (about 50% as judged from the refined atomic occupancy values; Figure 1B). Crystal growth requires 2–3 days, implying that the formation of the covalent bond can take place during crystallization. This finding allowed us to visualize the actual presence of a covalent bond between the protein and the cofactor, clearly supporting the idea that covalent bond formation with the flavin is not associated with any significant conformational alterations.

A minor but striking structural change that could be observed in the P15I/A394C structure involves Val433, which is pushed by 0.3 Å toward the N1–C2=O2 locus of the flavin ring, to establish a closer interaction which may be the cause of the improved FAD binding (Figure 2B). Given that in MAO B a Met is present at the position homologous to Val433 of PuO, we decided to generate A394C/V433M. We found that this double PuO mutant has indeed a significantly increased FAD:ADP ratio when compared to wild-type and A394C proteins (Table 2). This observation further supports the idea that minor alterations in the flavin environment can significantly alter its affinity to the protein cofactor site and change the levels of FAD versus ADP incorporation.

Table 2. Cofactor Distribution in PuO Variants and Amount of FAD Covalently Bound to the Monomers before and after FAD Covalent Incorporation

| | cofactor distribution in dimers (%) ^a | | | | % PuO monomers with FAD covalently bound ^b | |
|-------------------|--------------------------------------------------|-----------|------|---------------|-------------------------------------------------------|-----------------|
| | 2ADP | ADP + FAD | 2FAD | FAD:ADP ratio | as isolated | 48 h incubation |
| WT | 23.6 | 35.0 | 41.4 | 1.4 | 0 | 0 |
| A394C | 26.9 | 37.9 | 35.2 | 1.2 | 22 | 42 |
| P15I/A394C | 0 | 14.5 | 85.5 | 12.9 | 16 | 35 |
| A394C/V433M | 3.5 | 25.8 | 70.7 | 5.1 | 0 | nd ^c |
| A394C/A396T/Q431G | 22.6 | 38.9 | 38.6 | 1.4 | 40 | 56 |

^a The cofactor distribution in dimers was measured with ESI-MS under native conditions. ^b The amount of monomers with FAD covalently bound for freshly isolated enzyme was measured with ESI-MS in denaturing conditions and recalculated for monomers containing FAD and not ADP (based on ESI-MS in native conditions). The fractions of monomers with covalently bound FAD after 48 h incubation were measured with the TCA method. ^c nd = not determined.

Table 3. Steady-State Kinetic Parameters for PuO Variants with Putrescine as Substrate

| | <i>t</i> = 0 | | | <i>t</i> = 48 h | | |
|-------------------|--------------------------------------------|----------------------------|-------------------------------------------------------------------------------------|--------------------------------------------|----------------------------|-------------------------------------------------------------------------------------|
| | <i>k</i> _{cat} [s ^{−1}] | <i>K</i> _m [μM] | <i>k</i> _{cat} / <i>K</i> _m [s ^{−1} mM ^{−1}] | <i>k</i> _{cat} [s ^{−1}] | <i>K</i> _m [μM] | <i>k</i> _{cat} / <i>K</i> _m [s ^{−1} mM ^{−1}] |
| WT | 19.0 ± 0.6 | 45.4 ± 2.3 | 419 ± 21 | 8.8 ± 0.2 | 17.7 ± 0.4 | 497 ± 19 |
| A394C | 2.4 ± 0.1 | 19.7 ± 1.5 | 123 ± 9 | 2.4 ± 0 | 9.2 ± 0.6 | 261 ± 17 |
| P15I/A394C | 0.79 ± 0.01 | 13.4 ± 0 | 59 ± 1 | 0.78 ± 0.01 | 11.8 ± 1.5 | 67 ± 8 |
| A394C/A396T/Q431G | 0.95 ± 0.01 | 21.0 ± 1.4 | 45 ± 3 | 0.83 ± 0.01 | 13.7 ± 0.3 | 60 ± 1 |

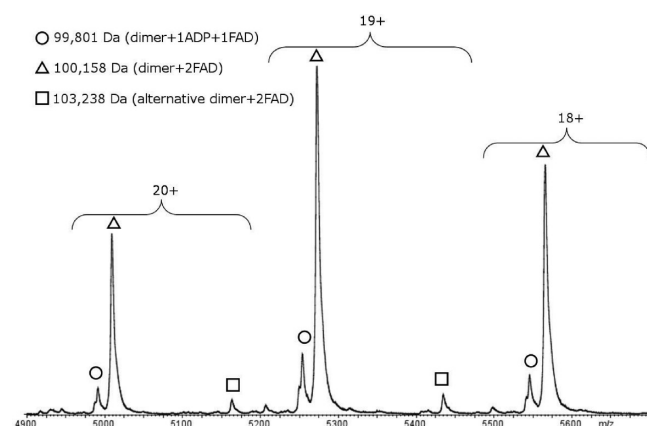


Figure 4. Mass spectrum of P15I/A394C PuO in its native state. Observed enzyme species are indicated with symbols and corresponding masses. The alternative dimer results from an alternative stop codon, as discussed in the Results section.

Improved Covalent FAD Incorporation: A394C/A396T/Q431G. To identify residues that hamper effective covalent flavinylation in PuO, we carefully analyzed the differences in active sites of PuO and MAO B. According to the proposed self-catalytic mechanism of covalent flavin attachment, the covalent coupling is initiated by proton abstraction from the C8α-methyl group of FAD (Figure 2) and/or from the residue forming the covalent bond with the flavin, suggesting that these deprotonations might limiting covalent flavinylation in PuO.^{3,7} Structural comparisons indicated that a Thr (Thr398) at a distance of 5.0 Å from the C8α-methyl group of flavin in MAO B is replaced by an Ala (Ala396) in PuO (Figure 5). A Thr at this position may facilitate covalent flavinylation by creating a more polar environment and/or

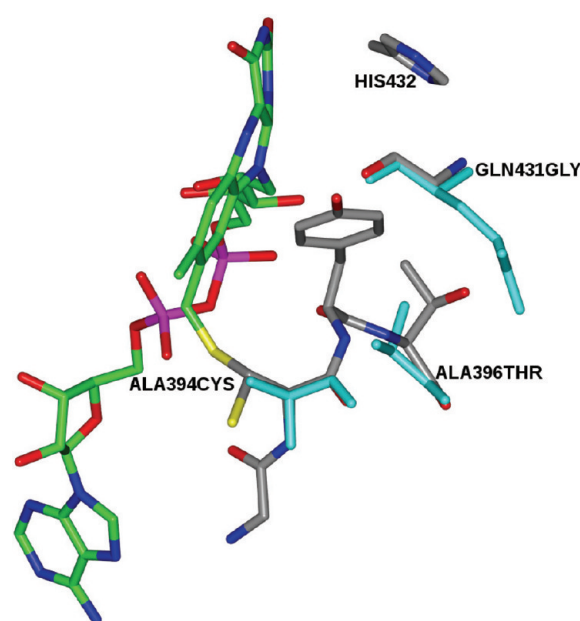


Figure 5. Comparison of the A394C/A396T/Q431G structure with that of the wild-type PuO (subunit B). Oxygens are in red, nitrogens in blue, and phosphorus atoms in magenta. The mutant carbon atoms are in gray whereas FAD carbons are in green. Wild-type Ala394, Ala396, and Gln431 are shown in cyan.

an H-bonding network that favors deprotonation of Cys394 or flavin C8α.⁹ However, further inspection of the PuO crystal structure reveals that a Thr side chain in position 396 would probably result in an unfavorable contact with the neighboring polar Gln431, which is a Gly in MAO-B. Therefore, we generated a triple mutant (A394C/A396T/Q431G) which was comparatively

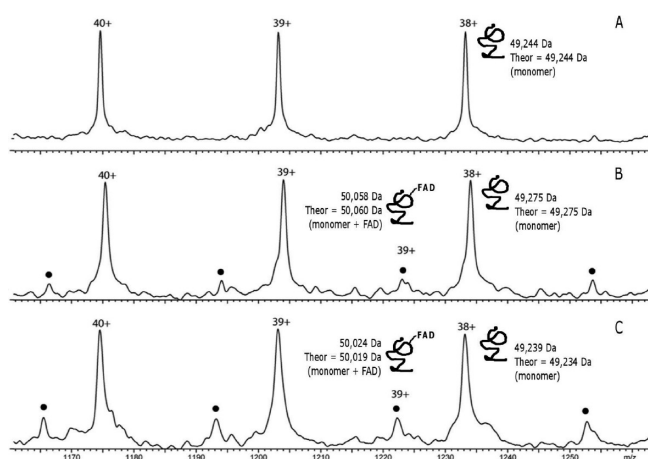


Figure 6. Mass spectra of denatured wild-type (A), A493C (B), and A394C/A396T/Q431G (C) PuO. Observed enzyme species with covalently bound FAD marked with a dot. Theoretical masses correspond to a monomer mass of the PuO variant minus N-terminal methionine.

analyzed by ESI-MS under denaturing conditions to quantify covalent flavinylation. Figure 6 shows the ESI-MS spectra of freshly purified wild-type, A394C, and A394C/A396T/Q431G proteins. Wild-type PuO shows only one species corresponding to the mass of PuO minus the N-terminal methionine (49 244 Da, the theoretical value). The mass spectrum of A394C reveals instead the presence of two species: 49 275 and 50 058 Da, corresponding to the calculated values of 49 275 and 50 060 Da for A394C without and with covalently bound FAD, respectively. Likewise, the mass spectrum of the denatured A394C/A396T/Q431G PuO also shows two major species: 49 239 and 50 024 Da, corresponding to the theoretical 49 234 and 50 019 Da, expected for the non-covalent and covalent forms of the mutant protein, respectively. However, the distribution of the two species differs between A394C and A394C/A396T/Q431G (Table 2). The triple mutant has a significantly higher degree of covalent FAD binding (40% covalent FAD) when compared to A394C PuO (22% covalent FAD). Clearly, the triple mutation favors formation of the covalent bond between Cys394 and FAD. However, the protein exhibits an overall (covalent and noncovalent) level of FAD incorporation similar to that of the wild-type protein as gathered from the similar values of FAD:ADP ratio measured by native ESI-MS (Table 2). This implies that the increased efficiency of flavin–protein covalent bond formation is not accompanied by an enhancement in affinity toward FAD compared to ADP.

The triple mutant crystal structure exhibits minor conformational changes, with the newly introduced side chains apparently causing little perturbations (Figure 5). A394C/A396T/Q431G was the only mutant protein to show somewhat less well-defined electron density for the flavin ring. This implies that the flavin site is not fully occupied (i.e., the crystalline proteins are partly in the ADP-bound form) or that there might be some disorder in the flavin conformation. Nevertheless, the electron density for subunit B shows that there is a partial (~50% occupancy) covalent attachment of the C8 α -methyl group of the flavin to Cys394, agreement with the enhanced efficiency of covalent flavinylation exhibited by the mutant, as indicated by ESI-MS spectra (Figure 6).

Kinetics of FAD Incorporation and Enzymatic Activities. In order to assess the time dependence of C8 α -cysteinylation

formation in PuO mutants, the covalent incorporation of FAD was monitored over time. To facilitate deprotonation and hence flavinylation, the experiments were performed at relatively high pH values. Enzyme stocks (210–460 μ M in 50 mM Tris-HCl, pH 7.5) were diluted in a 1:1 ratio with 50 mM sodium carbonate buffer, pH 10.0, containing 0.04% sodium azide. The enzyme solutions were incubated at 17 °C for 2 days, and the covalent FAD content and steady-state kinetics were measured at the beginning and at the end of the incubation (Table 3). In order to determine the amount of FAD covalently bound to the enzymes after 48 h, the TCA precipitation method was used. Flavin covalently bound to the protein will coprecipitate, whereas holo-proteins with noncovalently bound FAD will release the cofactor in solution upon denaturation. In this way, it is possible to estimate the ratio between covalent and noncovalent holoenzyme concentrations. As can be seen from Table 2, PuO mutants generally increase covalent incorporation of FAD during the incubation time, which is not observed for wild-type PuO. However, the process is very slow, and still not all FAD is covalently attached. The A394C/A396T/Q431G PuO is the most effective in flavin–protein covalent bond formation. After 2 days it covalently incorporates more than half of FAD. To further confirm this result, the mutant incubated for 3 days was analyzed by ESI-MS under denaturing conditions. The spectrum showed again two major peaks with the masses of 49 239 and 50 022 Da, corresponding to the theoretical (see above) masses of the monomer and the monomer with covalently bound FAD. The corrected value (the ratio between FAD and ADP did not change) for monomers with covalently bound FAD was 66%, which is in line with the value obtained with the TCA precipitation method (56% after 2 days). Steady-state kinetic parameters for putrescine were also determined before and after the incubation of the PuO variants (Table 3). It is apparent that wild-type PuO is somewhat more active than the mutants. Its catalytic efficiency ($k_{\text{cat}}/K_{\text{M}}$) is almost 4 times higher than that of A394C mutant and 8 times higher than those of the two other mutants. Interestingly, after 2 day incubation, the k_{cat} of wild-type PuO is half the original value, whereas it stays at the same level in the mutants. This finding suggests that covalent binding of FAD increases protein stability and maintenance of enzyme activity.

DISCUSSION

The crystal structures of PuO reveal that the enzyme possesses all the characteristic features of flavin–amine oxidases: an aromatic sandwich, a conserved pattern of interactions with the cofactor, a distorted nonplanar flavin, and a closed cavity for substrate binding, whose shape and H-bonding properties determine the substrate specificity^{9,10,20} (Figures 1–3). Compared to human MAOs, the most extensively studied members of the amine oxidase family, an interesting feature of PuO is that it lacks a covalent linkage between protein and the flavin ring. However, this property is not associated with any structural alterations within the cofactor-binding site, which is very similar to that of human MAOs. This includes the conservation of the *cis* peptide bond of the Tyr residue, that is part of the aromatic cage forming the binding site for the substrate amino group, i.e., the site of oxidation.²⁰ This finding suggests that this *cis* peptide is mainly necessary to attain the proper geometry in the active-site cavity and flavin binding region rather than for covalent flavinylation (Figure 2). On the other hand, such geometry is perfectly tailored to engage the flavin C8 α -methyl group in a covalent bond with

the protein. This is a “natural” event in MAOs whereas it can be “forced” to occur in PuO by site-directed mutagenesis, taking advantage of the apparent rigidity of the PuO’s cofactor site, which is seemingly preorganized for the effective introduction of the covalent protein–flavin bond. Indeed, the engineered PuO mutants, despite the introduced mutations, remain active, which shows that insertion/deletion of the covalent linkage is not essential for activity as found in other covalent flavoenzymes including MAO A.^{2,27}

A hypothesis underlying our studies was that by covalent tethering of FAD, the enzyme could fully incorporate the flavin cofactor, outcompeting the binding of ADP. However, the partially introduced covalent FAD did not result in any significant increase in the FAD incorporation into the enzyme (Table 2). This finding fully supports the proposal by Zhou et al., that the dinucleotide-binding motif provides a topological dock for the initial binding of FAD. Only after such a binding event, covalent bond formation can occur.²⁸ This is also in agreement with a study on NikD, a flavoprotein that takes part in nikkomycin biosynthesis and also belongs to the group of amine oxidases.²⁹ Significant amounts of ADP derivatives were found to be present in this protein, prohibiting full FAD binding. It has been suggested that the partial FAD binding is the result of heterologous over-expression. A limited FAD synthesis capacity of cells would lead to binding of cytosolic ADP and ADP derivatives, possibly upon misfolding of NikD. These observations suggest that the role of covalent flavinylation does not seem to be that of favoring incorporation of FAD compared to other mono- or dinucleotides that are potentially able to bind to the cofactor site on the protein.

Our studies on PuO also support the idea that covalent flavinylation is a self-catalytic process that critically depends on a proper FAD microenvironment.^{7,30–35} Indeed, the double P151/A394C mutant, which exhibits the highest FAD:ADP ratio, shows a poor level of covalent FAD binding, suggesting a suboptimal environment for covalent bond formation. Conversely, by introducing mutations predicted to alter the flavin C8 α environment (A394C/A396T/Q431G) the degree of covalent flavin attachment was increased (Table 2). The *in vitro* process of covalent flavinylation has been studied for several flavoenzymes by expressing the respective apo proteins in riboflavin auxotrophic expression strains. This has enabled the monitoring of the time-dependent covalent incorporation of flavin cofactors. Apo forms of these natural covalent flavoenzymes covalently anchor their FAD within several minutes (vanillyl alcohol oxidase³⁶ and monomeric sarcosine oxidase³⁷) or even hours (dimethylglycine dehydrogenase³⁸). Therefore, the slow formation of the covalent linkage observed in the PuO triple mutant is not exceedingly far from the slow flavinylation rates observed in certain natural covalent flavoproteins (Table 2). Altogether, these findings demonstrate that structure-based design of covalent flavinylation is feasible, although it may require several amino acid replacements, not necessarily confined to regions in direct contact with the flavin C8 α . Employment of flavoproteins for biocatalytic processes is often difficult because of their tendency to release FAD/FMN in the conditions of relevance for biocatalytic applications. The possibility of engineering flavoproteins to incorporate the cofactor through a covalent linkage will be critical to make progress in this area.

Accession Codes

Data depositions: coordinates and structure factors have been deposited with Protein Data Bank with entries 2yg3, 2yg4, 2yg5, 2yg6, and 2yg7.

AUTHOR INFORMATION

Corresponding Author

*E-mail m.w.fraaije@rug.nl. Tel +31503634345. Fax +3150 3634165.

Funding Sources

The financial support by the Italian Ministry of Science (PRIN08) and Fondazione Cariplo is gratefully acknowledged.

ACKNOWLEDGMENT

We gratefully acknowledge Arjan Barendregt for his support in ESI-MS experiments.

ABBREVIATIONS

PuO, putrescine oxidase from *Rhodococcus erythropolis*; MAO, monoamine oxidase; ESI, electrospray ionization; MS, mass spectrometry; TCA, trichloroacetic acid.

REFERENCES

- (1) Dym, O., and Eisenberg, D. (2001) Sequence-Structure Analysis of FAD-Containing Proteins. *Protein Sci.* 10, 1712–1728.
- (2) Heuts, D. P., Scrutton, N. S., McIntire, W. S., and Fraaije, M. W. (2009) What’s in a Covalent Bond? on the Role and Formation of Covalently Bound Flavin Cofactors. *FEBS J.* 276, 3405–3427.
- (3) Mewies, M., McIntire, W. S., and Scrutton, N. S. (1998) Covalent Attachment of Flavin Adenine Dinucleotide (FAD) and Flavin Mononucleotide (FMN) to Enzymes: The Current State of Affairs. *Protein Sci.* 7, 7–20.
- (4) Kim, J., Fuller, J. H., Kuusk, V., Cunane, L., Chen, Z. W., Mathews, F. S., and McIntire, W. S. (1995) The Cytochrome Subunit is Necessary for Covalent FAD Attachment to the Flavoprotein Subunit of p-Cresol Methylhydroxylase. *J. Biol. Chem.* 270, 31202–31209.
- (5) Brandsch, R., and Bichler, V. (1991) Autoflavinylation of apo 6-Hydroxy-D-Nicotine Oxidase. *J. Biol. Chem.* 266, 19056–19062.
- (6) Robinson, K. M., and Lemire, B. D. (1996) Covalent Attachment of FAD to the Yeast Succinate Dehydrogenase Flavoprotein Requires Import into Mitochondria, Presequence Removal, and Folding. *J. Biol. Chem.* 271, 4055–4060.
- (7) Trickey, P., Wagner, M. A., Jorns, M. S., and Mathews, F. S. (1999) Monomeric Sarcosine Oxidase: Structure of a Covalently Flavinylated Amine Oxidizing Enzyme. *Structure* 7, 331–345.
- (8) van Hellemond, E. W., van Dijk, M., Heuts, D. P., Janssen, D. B., and Fraaije, M. W. (2008) Discovery and Characterization of a Putrescine Oxidase from *Rhodococcus erythropolis* NCIMB 11540. *Appl. Microbiol. Biotechnol.* 78, 455–463.
- (9) Edmondson, D. E., Binda, C., Wang, J., Upadhyay, A. K., and Mattevi, A. (2009) Molecular and Mechanistic Properties of the Membrane-Bound Mitochondrial Monoamine Oxidases. *Biochemistry* 48, 4220–4230.
- (10) Atkin, K. E., Reiss, R., Koehler, V., Bailey, K. R., Hart, S., Turkenburg, J. P., Turner, N. J., Brzozowski, A. M., and Grogan, G. (2008) The Structure of Monoamine Oxidase from *Aspergillus niger* Provides a Molecular Context for Improvements in Activity obtained by Directed Evolution. *J. Mol. Biol.* 384, 1218–1231.
- (11) van Hellemond, E. W., Mazon, H., Heck, A. J., van den Heuvel, R. H., Heuts, D. P., Janssen, D. B., and Fraaije, M. W. (2008) ADP Competes with FAD Binding in Putrescine Oxidase. *J. Biol. Chem.* 283, 28259–28264.
- (12) DeSa, R. J. (1972) Putrescine Oxidase from *Micrococcus rubens*. Purification and Properties of the Enzyme. *J. Biol. Chem.* 247, 5527–5534.
- (13) Kearney, E. B., Salach, J. I., Walker, W. H., Seng, R. L., Kenney, W., Zeszotek, E., and Singer, T. P. (1971) The Covalently-Bound Flavin of Hepatic Monoamine Oxidase. I. Isolation and Sequence of a Flavin Peptide and Evidence for Binding at the 8 α Position. *Eur. J. Biochem.* 24, 321–327.

- (14) Collaborative Computational Project, Number 4. (1994) The CCP4 Suite: Programs for Protein Crystallography. *Acta Crystallogr., Sect. D: Biol. Crystallogr.* 50, 760–763.
- (15) Emsley, P., Lohkamp, B., Scott, W. G., and Cowtan, K. (2010) Features and Development of Coot. *Acta Crystallogr., Sect. D: Biol. Crystallogr.* 66, 486–501.
- (16) Potterton, L., McNicholas, S., Krissinel, E., Gruber, J., Cowtan, K., Emsley, P., Murshudov, G. N., Cohen, S., Perrakis, A., and Noble, M. (2004) Developments in the CCP4 Molecular-Graphics Project. *Acta Crystallogr., Sect. D: Biol. Crystallogr.* 60, 2288–2294.
- (17) Kleywegt, G. J., and Jones, T. A. (1994) Detection, Delineation, Measurement and Display of Cavities in Macromolecular Structures. *Acta Crystallogr., Sect. D: Biol. Crystallogr.* 50, 178–185.
- (18) Son, S. Y., Ma, J., Kondou, Y., Yoshimura, M., Yamashita, E., and Tsukihara, T. (2008) Structure of Human Monoamine Oxidase A at 2.2-Å Resolution: The Control of Opening the Entry for substrates/inhibitors. *Proc. Natl. Acad. Sci. U.S.A.* 105, 5739–5744.
- (19) Berman, H. M., Westbrook, J., Feng, Z., Gilliland, G., Bhat, T. N., Weissig, H., Shindyalov, I. N., and Bourne, P. E. (2000) The Protein Data Bank. *Nucleic Acids Res.* 28, 235–242.
- (20) Binda, C., Mattevi, A., and Edmondson, D. E. (2002) Structure-Function Relationships in Flavoenzyme-Dependent Amine Oxidations: A Comparison of Polyamine Oxidase and Monoamine Oxidase. *J. Biol. Chem.* 277, 23973–23976.
- (21) Binda, C., Angelini, R., Federico, R., Ascenzi, P., and Mattevi, A. (2001) Structural Bases for Inhibitor Binding and Catalysis in Polyamine Oxidase. *Biochemistry* 40, 2766–2776.
- (22) Li, M., Binda, C., Mattevi, A., and Edmondson, D. E. (2006) Functional Role of the “Aromatic Cage” in Human Monoamine Oxidase B: Structures and Catalytic Properties of Tyr435 Mutant Proteins. *Biochemistry* 45, 4775–4784.
- (23) Wierenga, R. K., De Maeyer, M. C. H., and Hol, W. G. J. (1985) Interaction of Pyrophosphate Moieties with α -Helices in Dinucleotide-Binding Proteins. *Biochemistry* 24, 1346–1357.
- (24) Vallon, O. (2000) New Sequence Motifs in Flavoproteins: Evidence for Common Ancestry and Tools to Predict Structure. *Proteins* 38, 95–114.
- (25) Trickey, P., Basran, J., Lian, L. Y., Chen, Z., Barton, J. D., Sutcliffe, M. J., Scrutton, N. S., and Mathews, F. S. (2000) Structural and Biochemical Characterization of Recombinant Wild Type and a C30A Mutant of Trimethylamine Dehydrogenase from *Methylophilus methylotrophus* (Sp. W(3)A(1)). *Biochemistry* 39, 7678–7688.
- (26) van den Heuvel, R. H., and Heck, A. J. (2004) Native Protein Mass Spectrometry: From Intact Oligomers to Functional Machineries. *Curr. Opin. Chem. Biol.* 8, 519–526.
- (27) Miller, J. R., and Edmondson, D. E. (1999) Influence of Flavin Analogue Structure on the Catalytic Activities and Flavinylation Reactions of Recombinant Human Liver Monoamine Oxidases A and B. *J. Biol. Chem.* 274, 23515–23525.
- (28) Zhou, B. P., Lewis, D. A., Kwan, S. W., and Abell, C. W. (1995) Flavinylation of Monoamine Oxidase B. *J. Biol. Chem.* 270, 23653–23660.
- (29) Bruckner, R. C., Zhao, G., Ferreira, P., and Jorns, M. S. (2007) A Mobile Tryptophan is the Intrinsic Charge Transfer Donor in a Flavoenzyme Essential for Nikkomycin Antibiotic Biosynthesis. *Biochemistry* 46, 819–827.
- (30) Walsh, C. (1980) Flavin Coenzymes: At the Crossroads of Biological Redox Chemistry. *Acc. Chem. Res.* 13, 148–155.
- (31) Efimov, I., and McIntire, W. S. (2004) A Study of the Spectral and Redox Properties and Covalent Flavinylation of the Flavoprotein Component of p-Cresol Methylhydroxylase Reconstituted with FAD Analogues. *Biochemistry* 43, 10532–10546.
- (32) Koetter, J. W., and Schulz, G. E. (2005) Crystal Structure of 6-Hydroxy-D-Nicotine Oxidase from *Arthrobacter nicotinovorans*. *J. Mol. Biol.* 352, 418–428.
- (33) Weyler, W., Hsu, Y. P., and Breakefield, X. O. (1990) Biochemistry and Genetics of Monoamine Oxidase. *Pharmacol. Ther.* 47, 391–417.
- (34) Hirashiki, I., Ogata, F., and Ito, A. (1995) Rat Monoamine Oxidase B Expressed in *Escherichia coli* has a Covalently-Bound FAD. *Biochem. Mol. Biol. Int.* 37, 39–44.
- (35) Lu, G., Unger, T., Owerla-Atepo, J. B., Shih, J. C., Ekblom, J., and Orelund, L. (1996) Characterization and Partial Purification of Human Monoamine Oxidase-B Expressed in *Escherichia coli*. *Protein Expression Purif.* 7, 315–322.
- (36) Jin, J., Mazon, H., van den Heuvel, R. H., Heck, A. J., Janssen, D. B., and Fraaije, M. W. (2008) Covalent Flavinylation of Vanillyl-Alcohol Oxidase is an Autocatalytic Process. *FEBS J.* 275, 5191–5200.
- (37) Hassan-Abdallah, A., Bruckner, R. C., Zhao, G., and Jorns, M. S. (2005) Biosynthesis of Covalently Bound Flavin: Isolation and in Vitro Flavinylation of the Monomeric Sarcosine Oxidase Apoprotein. *Biochemistry* 44, 6452–6462.
- (38) Brizio, C., Brandsch, R., Douka, M., Wait, R., and Barile, M. (2008) The Purified Recombinant Precursor of Rat Mitochondrial Dimethylglycine Dehydrogenase Binds FAD Via an Autocatalytic Reaction. *Int. J. Biol. Macromol.* 42, 455–462.